Semiconductor Physics, Quantum Electronics & Optoelectronics, 2022. V. 25, No 3. P. 275-281.

Semiconductor physics

Continuous wave and pulsed EPR study of $Cd_{1-x}Mn_xTe$ crystals with different Mn content

D.V. Savchenko[1,2,*], M.K. Riasna[1], M.V. Chursanova[1], T.V. Matveeva[1], N.A. Popenko[3], I.V. Ivanchenko[3], E.N. Kalabukhova[4]

[1]*National Technical University of Ukraine "Igor Sikorsky Kyiv Polytechnic Institute"*
37, prosp. Peremohy, 03056 Kyiv, Ukraine
[2]*Institute of Physics of the CAS, 2 Na Slovance, 182 21 Prague, Czech Republic*
[3]*O. Usikov Institute for Radiophysics and Electronics, NAS of Ukraine*
12, Proskura str., 61085 Kharkiv, Ukraine
[4]*V. Lashkaryov Institute of Semiconductor Physics, NAS of Ukraine*
41, prosp. Nauky, 03680 Kyiv, Ukraine
**Corresponding author e-mail: dariyasavchenko@gmail.com*

Abstract. The cadmium manganese telluride ($Cd_{1-x}Mn_xTe$) crystals ($x < 0.001$ and $x = 0.02$, 0.04, 0.1) grown using the Bridgman method were studied by applying continuous wave and pulsed electron paramagnetic resonance (EPR) spectroscopy in the wide temperature range. The $Cd_{1-x}Mn_xTe$ crystals with $x < 0.001$ revealed the EPR spectrum from isolated Mn^{2+} with $g_\perp = g_\parallel = 2.0074(3)$, $|A|_\perp = |A|_\parallel = 56.97 \cdot 10^{-4}$ cm^{-1}, $|a| = 30.02 \cdot 10^{-4}$ cm^{-1}, while $Cd_{1-x}Mn_xTe$ crystals with $x = 0.02 \ldots 0.04$ are characterized by two single broad isotropic EPR lines of Lorentzian shape ($g \sim 2.009$ and $g \sim 1.99$) due to Mn clusters of different sizes. The EPR spectrum of $Cd_{1-x}Mn_xTe$ crystals with $x = 0.01$ consists of the single broad line at $g \sim 2.01$ due to higher level of homogeneity inherent to these crystals. The temperature dependence of spin relaxation times for the isolated Mn^{2+} center in the $Cd_{1-x}Mn_xTe$ crystals with $x < 0.001$ has been described using the conceptions of Orbach process for T_M^{-1} and two-phonon Raman process for T_1^{-1}.

Keywords: EPR, spin relaxation time, manganese, cadmium manganese telluride.

https://doi.org/10.15407/spqeo25.03.275
PACS 61.72.Hh, 76.30.-v

Manuscript received 16.05.22; revised version received 09.08.22; accepted for publication 21.09.22; published online 06.10.22.

1. Introduction

Cadmium manganese telluride ($Cd_{1-x}Mn_xTe$) is a modern semiconductor material used for application in room-temperature X- and γ-ray detectors. Due to these advantages, namely: tunable wide bandgap, high resistivity and good carrier transport properties [1], $Cd_{1-x}Mn_xTe$ has recently revealed the ability to substitute the existing Cd(Zn)Te detector crystals [2–4].

Despite numerous studies of $Cd_{1-x}Mn_xTe$ crystals by using different experimental techniques, the electron paramagnetic resonance (EPR) spectroscopy data of this material are still presented less. In particular, there is a discrepancy in interpretation of EPR data for isolated Mn^{2+} in $Cd_{1-x}Mn_xTe$ crystals. As it was reported in [5], the EPR spectrum of Mn^{2+} in CdTe:Mn crystals consists of five sextets of hyperfine lines with the splitting between these sextets specified by the large cubic crystal field coefficient ($28 \cdot 10^{-4}$ cm^{-1}) that was related to an unusually large cubic field splitting effect. Recently, the appearance of additional lines in the Mn^{2+} EPR spectrum with temperature decrease was attributed to the superhyperfine interaction of $3d^5$-electrons of Mn^{2+} with nuclear moments of ^{125}Te and ^{123}Te isotopes [6]. However, no detailed analysis of angular dependence of EPR spectra and relative intensity ratio of EPR lines were presented in [6].

In [7], the temperature dependence of the spin-lattice relaxation time for Mn^{2+} in the $Cd_{1-x}Mn_xTe$ crystals with $x = 0.005$, 0.01 and 0.02 have been studied. Furthermore, in [5] the authors reported the value of spin-lattice relaxation time for the Mn^{2+} in CdTe:Mn crystals containing 0.01% of Mn at 300, 77 and 4.2 K only. However, no detailed study was presented for the temperature behavior of the spin relaxation times for Mn^{2+} in the $Cd_{1-x}Mn_xTe$ crystals with $x < 0.001$.

In this work, we report the results of detailed studying the Mn^{2+} in $Cd_{1-x}Mn_xTe$ crystals with $x < 0.1$ by using the continuous wave (CW) and pulsed EPR techniques. The spin-Hamiltonian parameters were taken from the angular dependence of isolated Mn^{2+} EPR spectra in the $Cd_{1-x}Mn_xTe$ crystals with $x < 0.001$, and it was proved that the observed EPR spectrum is related to the crystal-field splitting of Mn^{2+}. The temperature dependence of phase memory time and spin-lattice relaxation time for isolated Mn^{2+} in the $Cd_{1-x}Mn_xTe$ crystals with $x < 0.001$ measured at $T < 50$ K was described in the framework of Orbach and two-phonon Raman processes, correspondingly. The EPR spectra of $Cd_{1-x}Mn_xTe$ crystals with $x = 0.02$, 0.04, 0.1 consist of the broad single lines related to Mn clusters of different sizes.

2. Materials and methods

The $Cd_{1-x}Mn_xTe$ crystals with $x < 0.001$ ($N_{Mn} \approx 10^{19}$ cm^{-3}), $x = 0.02$, 0.04, 0.1 were grown using the vertical Bridgman method. The crystals were cut along the (110) plane with the size 6×3×1 mm.

The CW and pulsed EPR measurements were performed using the X-band Bruker ELEXSYS E580 spectrometer. For CW EPR experiments, the ER 4122 SHQE SuperX High-Q cavity equipped with ER 4112HV variable temperature helium-flow cryostat was used. For pulsed EPR measurements, we used the EN 4118X-MD5 cavity equipped with the cryostat ER 4118CF.

The experimental parameters for CW EPR were set as follows: microwave power level was 0.05 mW, modulation frequency 100 kHz, modulation amplitude 0.4…1 mT (depending on the EPR linewidth), conversion time 60 ms. The standard DPPH free radical with $g = 2.0036$ was used as a reference sample. Electron spin echo (ESE) decay traces were recorded using the primary echo sequence, $\pi/2 - \tau - \pi - \tau -$ echo, by increasing the interpulse delay τ of the primary echo sequence with the pulse lengths: $\pi/2 = 16$ ns, $\tau = 800$ ns, $\pi = 32$ ns with the short repetition time of 4 μs. ESE inversion-recovery experiment was performed using three-pulse sequence: $\pi - T - \pi/2 - \tau - \pi - \tau -$echo with $\pi = 30$ ns, $T = 400$ ns, $\pi/2 = 16$ ns, $\tau = 400$ ns, $\pi = 32$ ns with the short repetition time of 6 μs.

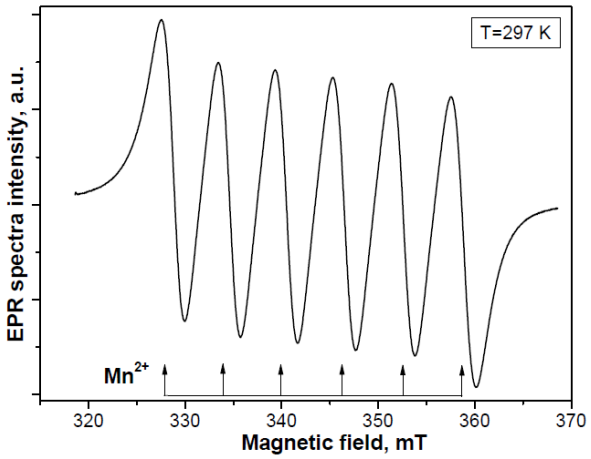

Fig. 1. EPR spectrum measured in the $Cd_{1-x}Mn_xTe$ crystals with $x < 0.001$ at $T = 297$ K. $\vec{B} \| \vec{c}$.

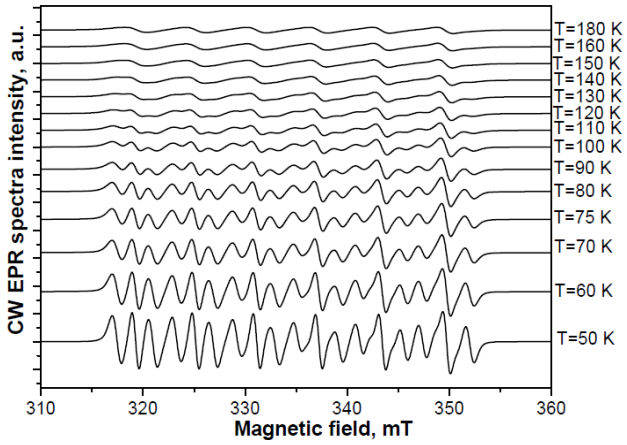

Fig. 2. Temperature dependence for the EPR spectrum of Mn^{2+} in the measured $Cd_{1-x}Mn_xTe$ crystals with $x < 0.001$ within the temperature range from 180 down to 50 K. $\vec{B} \| \vec{c}$.

3. Results and discussion

3.1. EPR spectra in the $Cd_{1-x}Mn_xTe$ crystals with $x < 0.001$

Six lines due to the hyperfine coupling with ^{55}Mn nuclei ($I = 5/2$, 100% abundance) was observed in the $Cd_{1-x}Mn_xTe$ crystals with $x < 0.001$ at $T = 297$ K (Fig. 1). This sextet of lines is centered at $g = 2.0074(2)$, and the hyperfine splitting of 6.1 mT corresponds to the Mn^{2+} ($S = 5/2$).

Fig. 2 shows the temperature dependence of EPR spectra measured in the $Cd_{1-x}Mn_xTe$ crystals with $x < 0.001$ within the temperature range from 180 down to 50 K. At $T < 180$ K, the width of sextet lines starts to decrease, and additional lines appear in the spectrum. At $T < 50$ K, the EPR spectrum reveals its "saturation" effect due to the prolongation of the spin-lattice relaxation time for Mn^{2+} with decreasing the temperature.

Fig. 3 shows the angular dependence of EPR spectra measured in the $Cd_{1-x}Mn_xTe$ crystals with $x < 0.001$ at $T = 50$ K, when the crystal rotates around the $\vec{c}$ axis. The angular dependence shows that the main line of this sextet is isotropic, while the additional lines reveal a significant angular dependence.

It is well known that the EPR spectrum of Mn^{2+} in trigonal symmetry should be described by the following spin Hamiltonian [8–10]:

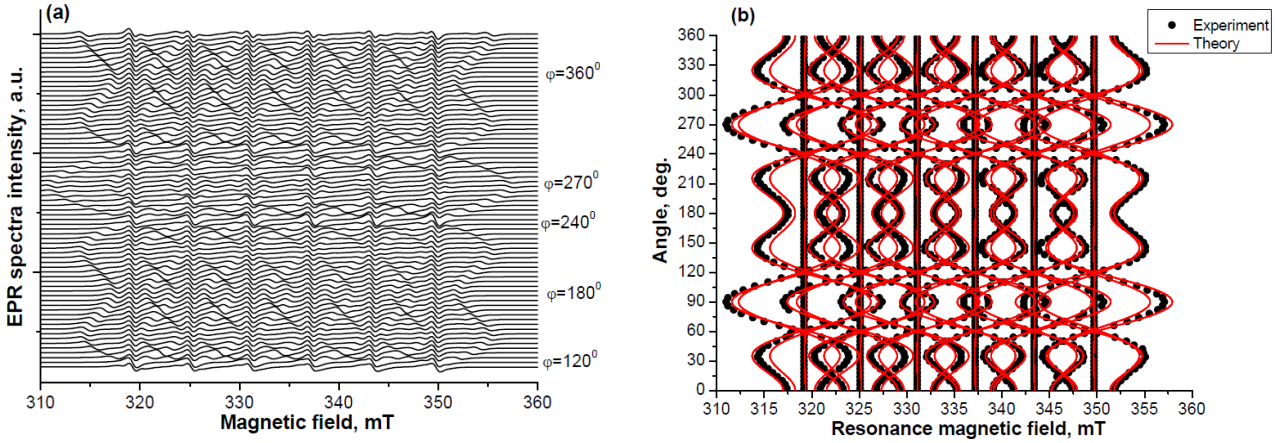

Fig. 3. Angular dependence of EPR spectra (a) and resonance magnetic field values (b) measured in $Cd_{1-x}Mn_xTe$ crystals with $x < 0.001$ at $T = 50$ K, when the crystal rotates around the $\vec{c}$ axis. Black dots are experimental data, and solid red lines are the result of modeling by using Eq. (1).

$$H_0 = g_{||}\mu_B B_z S_z + g_{\perp}\mu_B\left(B_x S_x + B_y S_y\right) +$$
$$+ D\left[S_z^2 - \frac{1}{3}S(S+1)\right] +$$
$$+ \frac{a}{6}\left[S_x^4 + S_y^4 + S_z^4 - \frac{1}{5}(S+1)\left(3S^2+3S-1\right)\right] +$$
$$+ \frac{F}{180}\left[\begin{array}{l} 35S_z^4 - 30S(S+1)S_z^2 + 25S_z^2 - 6S(S+1) + \\ + 3S^2(S+1)^2 \end{array}\right] +$$
$$+ A_{||}S_z I_z + A_{\perp}\left(S_x I_x + S_y I_y\right) + Q\left[I_z^2 - \frac{1}{3}I(I+1)\right] -$$
$$- g_N\mu_N \vec{B}\cdot\vec{I},$$

where $g_{||}$, $g_{\perp}$ – components of $\vec{g}$ -tensor of spectroscopic splitting, g_N – nuclear g-factor, μ_B – Bohr magneton, μ_N – nuclear magneton, $\vec{B}$ – applied magnetic field, $D = 3B_2^0$ – second-order spin operator, representing a component of the crystalline electric field that is axially symmetric about the **c**-axis, $a = 24B_4^4$ – fourth-order spin operator, representing the cubic component of crystalline electric field, $F = 180B_4^0 - 36B_4^4$ – fourth-order spin operator, representing the component of crystalline electric field that is axially symmetric about the $\vec{c}$ -axis, $A_{||}$, $A_{\perp}$ – components of hyperfine interaction tensor, Q – nuclear quadrupole moment, I – nuclear spin, S – electron spin.

To determine the spin-Hamiltonian parameters for the Mn^{2+} center in $Cd_{1-x}Mn_xTe$ crystal from the angular dependence of resonance magnetic field values, simulation of this angular dependence was performed using the Easyspin 5.2.28 module [11] and the spin Hamiltonian (1).

The simulated angular dependences for Mn^{2+} in the $Cd_{1-x}Mn_xTe$ crystal (Fig. 3b) were obtained with the parameters listed in Table. As it follows from this Table, the obtained data agree well with the spin-Hamiltonian parameters for Mn^{2+} in $Cd_{1-x}Mn_xTe$ presented in [5]. Therefore, the appearance of additional lines in the EPR spectrum at $T < 180$ K in the $Cd_{1-x}Mn_xTe$ crystals with $x < 0.001$ should be unambiguously attributed to the crystal-field splitting of Mn^{2+} levels.

At $T < 50$ K, we have studied the temperature dependence of spin-relaxation times inherent to Mn^{2+} in the $Cd_{1-x}Mn_xTe$ crystals with $x < 0.001$ by using pulsed EPR techniques. Fig. 4 shows the temperature dependence of phase memory and spin-lattice relaxation rates for Mn^{2+} in the $Cd_{1-x}Mn_xTe$ crystals with $x < 0.001$.

From ESE decay traces measured at the magnetic field position of the Mn^{2+} center that were fitted to the stretched exponential function, we obtained the phase memory time (T_M):

$$I(t) = I(0)\exp\left(-t/T_M\right), \qquad (3)$$

where $I(t)$ is the ESE intensity at time t. From the analysis of ESE decay traces, we obtained that $T_M = 349$ s at $T = 5$ K.

Table. The spin-Hamiltonian parameters for Mn^{2+} in the $Cd_{1-x}Mn_xTe$ crystals and films obtained in this work at $T = 50$ K and that of literature.

$g_{\perp}$	$g_{||}$	$\|A\|_{\perp}\cdot10^{-4}$, cm^{-1}	$\|A\|_{||}\cdot10^{-4}$, cm^{-1}	$\|a\|\cdot10^{-4}$, cm^{-1}	Reference
2.0074(3)	2.0074(3)	56.97	56.97	30.02	This work
2.010	2.010	55	55	28	[5]
2.0079	2.0079	56.7	56.7	18	[12]
2.0090	2.0090	59.9(2)	59.9(2)		[13]

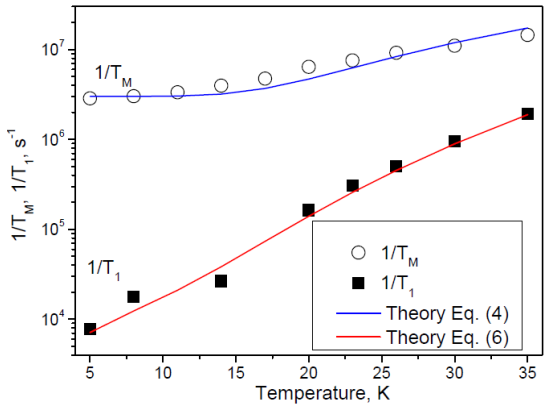

Fig. 4. Temperature dependence of T_M^{-1} (open circles) and T_1^{-1} (black squares) rates for Mn^{2+} in the $Cd_{1-x}Mn_xTe$ crystals with $x < 0.001$. Blue and red lines represent the result of fitting by using Eqs (4) and (6), respectively.

We found that the temperature dependence of the T_M^{-1} rate for the Mn^{2+} center shown in Fig. 4 agrees well with the following equation:

$$T_M^{-1}(T) = T_{M,0}^{-1} + c\exp(-\Delta/kT), \quad (4)$$

where $T_{M,0}^{-1}$ is the temperature-independent contribution from spectral diffusion, and the exponential term describes contribution from libration motion *via* the energy barrier Δ or/and a contribution from excitations to the higher energy level by the value Δ. The fitting of Eq. (3) with experimental data gives the following values of parameters: $T_{M,0}^{-1} = 3\cdot10^6$ s^{-1}, Δ = 8.62 meV = 100 K, $c = 2.5\cdot10^8$ s^{-1}.

The spin-lattice relaxation time (T_1) was determined from a fit of the echo inversion-recovery amplitude measured at the magnetic field position of the Mn^{2+} center with the biexponential function:

$$I_{echo}(t) = I_1\exp(-t/T_1) + I_{SD}\exp(-t/T_{SD}), \quad (5)$$

where I_1 and I_{SD} are amplitudes, and T_{SD} is the time of spectral diffusion that affects the inversion recovery pulse sequence. Therefore, only the slower component T_1 was considered. From the analysis of the experimental data, and we obtained that $T_1 = 1.29\cdot10^5$ s at $T = 5$ K.

The temperature dependence of the T_1^{-1} rate for the Mn^{2+} center shown in Fig. 4 is described well by the two-phonon Raman process:

$$T_1^{-1}(T) = aT + bT^5, \quad (6)$$

where a and b are the coefficients depending on the details of relaxation mechanism.

From the fitting of Eq. (5) with experimental data in Fig. 4, we found that $a = 1400$ K^{-1}·s^{-1} and $b = 0.035$ K^{-5}·s^{-1}.

3.2. EPR spectra in the $Cd_{1-x}Mn_xTe$ crystals with $x > 0.01$

At room temperature, the $Cd_{1-x}Mn_xTe$ crystals with x = 0.02, 0.04, 0.1 revealed a broad line centered at $g \sim 2.009\ldots2.01$ and with the linewidth (ΔB_{pp}) ranging from 10 mT (x = 0.02, 0.04) up to 35 mT (x = 0.1). At low temperatures, this line broadens dramatically and in the $Cd_{1-x}Mn_xTe$ crystals with x = 0.02, 0.04 an additional less intense line at $g \sim 1.99$ with a linewidth of 7 mT appears (see Fig. 5). The g-factor and linewidth for both EPR signals turned out to be isotropic.

The EPR spectra of $Cd_{1-x}Mn_xTe$ crystals with $x > 0.01$ did not reveal any sextet of lines from Mn^{2+}, since it can be observed only when the linewidth of individual lines is less than their hyperfine interaction constant. It is known that the dipolar coupling between Mn^{2+} ions leads to the EPR line broadening. As a result, the molecular field acts on the Mn^{2+} ions to vary from one site to another by shifting the resonance frequency of the different Mn^{2+} ions [14]. This mechanism leads to the transformation of the Mn^{2+} sextet to a single inhomogeneous broadened EPR line in fne $Cd_{1-x}Mn_xTe$, when $x > 0.002$.

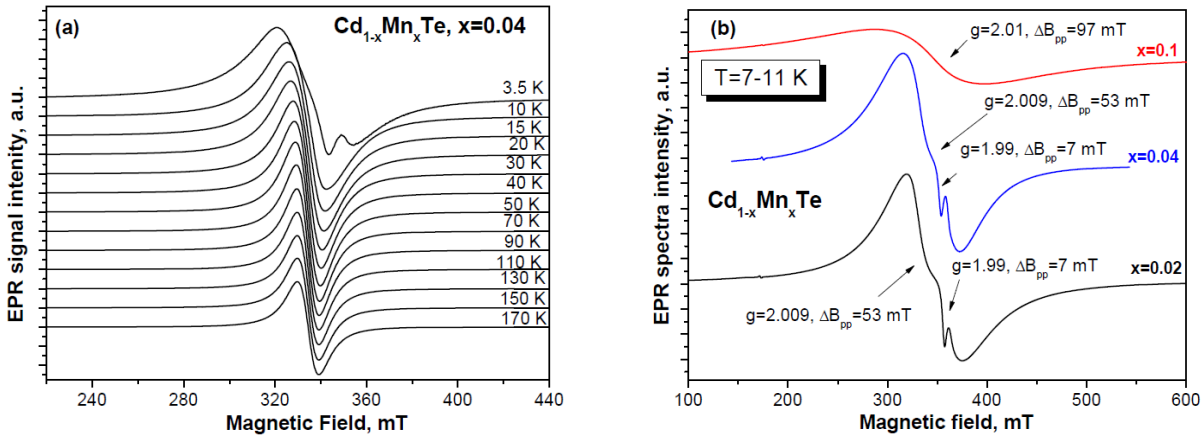

Fig. 5. Temperature dependence of EPR spectra observed in the $Cd_{1-x}Mn_xTe$ crystals with x = 0.04 (a). The EPR spectra measured in the $Cd_{1-x}Mn_xTe$ crystals with x = 0.02, 0.04, 0.1 at T = 7…11 K (b).

It can be seen from Fig. 5b that there are two lines in the EPR spectrum of $Cd_{1-x}Mn_xTe$ crystals with x = 0.02…0.04: the broad and narrow ones. The appearance of those two lines can be explained by a cluster model suggested in [15] and applied to $Cd_{1-x}Mn_xTe$ crystals in [16]. According to [16], fluctuations in the Mn content lead to the appearance of clusters of two types. The larger clusters have Mn content close to the x-value, and smaller clusters have lower Mn content. The broad EPR line should be attributed to the larger clusters, while the narrow line belongs to the smaller ones. The absence of the narrow line in the EPR spectra of $Cd_{1-x}Mn_xTe$ crystals with x = 0.1 may indicate a higher level of homogeneity inherent to these crystals.

The observed line broadening of the broad intense EPR line at T < 50 K can be caused by the effect of anisotropic superexchange interaction between Mn^{2+} ions [17].

4. Conclusions

We have studied the $Cd_{1-x}Mn_xTe$ crystals grown using the vertical Bridgman method with different Mn concentrations by using the CW and pulsed EPR methods. At T < 180 K, the width of the Mn^{2+} sextet lines in the $Cd_{1-x}Mn_xTe$ crystals with x < 0.001 starts to decrease, and additional lines in the EPR spectrum appear. Fitting the spin Hamiltonian for Mn^{2+} in trigonal symmetry with experimental data allowed us to obtain the following parameters for Mn^{2+} in the $Cd_{1-x}Mn_xTe$ crystals with x < 0.001: $g_\perp = g_\parallel$ = 2.0074(3), $|A|_\perp = |A|_\parallel$ = $56.97 \cdot 10^{-4}$ cm^{-1}, $|a|$ = $30.02 \cdot 10^{-4}$ cm^{-1}. The temperature dependence of phase memory rate for Mn^{2+} in the $Cd_{1-x}Mn_xTe$ crystals with x < 0.001 was described using the Orbach process conception with Δ = 8.62 meV, while the temperature dependence of the spin-lattice relaxation rate was fitted with two-phonon Raman process.

The EPR spectra of $Cd_{1-x}Mn_xTe$ crystals with x = 0.02, 0.04 consisted of two signals: one intense broad line at g ~ 2.009 and a less intense and narrow one at g ~ 1.99. The intense line was attributed to the larger Mn clusters, and the narrow line is related to the smaller ones that appeared due to fluctuations in the Mn content. The absence of a narrow line in the EPR spectra of $Cd_{1-x}Mn_xTe$ crystals with x = 0.1 can be explained by a higher level of homogeneity in these crystals

Acknowledgments

This research was supported by Operational Program Research, Development and Education financed by European Structural and Investment Funds and the Czech Ministry of Education, Youth and Sports [Project SOLID21 CZ.02.1.01/0.0/0.0/16_019/0000760].

References

1. Yu P., Jiang B., Liu W., Shao T., Gao P. Research progress on postgrowth annealing of $Cd_{1-x}Mn_xTe$ crystals. *Cryst. Res. Technol.* 2022. P. 2200007 (Early View). https://doi.org/10.1002/crat.202200007.
2. Yu P., Xu Y., Chen Y. *et al*. Investigation of effective annealing on CdMnTe:In crystals with different thickness for gamma-ray detectors. *J. Cryst. Growth*. 2018. **483**. P. 94–101. https://doi.org/10.1016/j.jcrysgro.2017.11.012.
3. Nykoniuk Y., Solodin S., Zakharuk Z. *et al*. Compensated donors in semi-insulating $Cd_{1-x}Mn_xTe$:In crystals. *J. Cryst. Growth*. 2018. **500**. P. 117–121. https://doi.org/10.1016/j.jcrysgro.2018.08.013.
4. Brovko A., Rusian P., Chernyak L., Ruzin A. High quality planar $Cd_{1-x}Mn_xTe$ room-temperature radiation detectors. *Appl. Phys. Lett.* 2021. **119**. No 6. P. 062103-1–062103-4. https://doi.org/10.1063/5.0060706.
5. Lambe J., Kikuchi C. Paramagnetic resonance of CdTe:Mn and CdS:Mn. *Phys. Rev*. 1960. **119**, No 4. P. 1256–1260. https://doi.org/10.1103/PhysRev.119.1256.
6. Plyatsko S.V., Gromovyi Y.S., Stril'chuk O.M. *et al*. Laser-induced point defects in CdTe:Mn single crystals irradiated by IR laser. *J. Nano-Electron. Phys.* 2019. **11**, No 6. P. 06005-1–06005-5. https://doi.org/10.21272/jnep.11(6).06005.
7. Scalbert D., Cernogora J., La Guillaume C.B.A. Spin-lattice relaxation in paramagnetic CdMnTe. *Solid State Commun.* 1988. **66**, No 6. P. 571–574. https://doi.org/10.1016/0038-1098(88)90210-4.
8. Jain V.K., Lehmann G. Electron paramagnetic resonance of Mn^{2+} in orthorhombic and higher symmetry crystals. *phys. status solidi* (*b*). 1990. **159**. P. 495–544. https://doi.org/10.1002/pssb.2221590202.
9. Vinokurov V.M., Zaripov M.M., Stepanov V.G. A study of some Mn containing carbonates by the method of electron paramagnetic resonance. *Sov. Phys. Crystal.* 1961. **6**. P. 104–108.
10. Bleaney B., Ingram D.E. The paramagnetic resonance spectra of two salts of manganese. *Proc. R. Soc. A.: Math. Phys. Eng. Sci*. 1951. **205**, No 1082. P. 336–356. https://doi.org/10.1098/rspa.1951.0033.
11. Stoll S., Schweiger A. EasySpin, a comprehensive software package for spectral simulation and analysis in EPR. *J. Magn. Reson*. 2006. **178**, No 1. P. 42–55. https://doi.org/10.1016/j.jmr.2005.08.013.
12. Nakamura T., Hayashi K., Nakanishi Y. *et al*. Manganese(II) in superlattices consisting of alternate cadmium telluride and zinc sulfide layers. *J. Chem. Soc. Faraday Trans*. 1996. **92**, No 21. P. 4247–4250. https://doi.org/10.1039/FT9969204247.
13. Yavorsky Y.V., Zaulichny Y.V., Gunko V.M., Karpets M.V. Influence of mechanical treatment on structural and morphological characteristics and distribution of valence electrons of aluminum, silicon, iron and titanium oxides. *J. Nano-Electron. Phys.* 2018. **10**, No. 6. P. 06005-1–06005-8. https://doi.org/10.21272/jnep.10(6).06005.

14. Gad S.A., Boshta M., Moustafa A.M. *et al*. Structural, optical, magnetic and electrical properties of dilute magnetic semiconductor $Cd_{1-x}Mn_xTe$. *Solid State Sci.* 2011. **13**, No 1. P. 23–29. http://doi.org/10.1016/j.solidstatesciences.2010.09.022.
15. Šoškić Z., BabićStojić B. Cluster method analysis of the EPR line in $Zn_{1-x}Mn_xTe$. *J. Magn. Magn. Mater*. 1995. **140**–**144**, Part 3. P. 2071–2073. https://doi.org/10.1016/0304-8853(94)01209-1.
16. Partyka J., Żukowski P.W., Wegierek P. *et al*. Electron spin resonance in $Cd_{1-x}Mn_xTe$ and $Zn_{1-x}Mn_xTe$ compounds. *Semiconductors.* 2002. **36**, No 12. P. 1347–1351. https://doi.org/10.1134/1.1529244.
17. Soskic Z., Stojic B.B., Stojic M. Electron paramagnetic resonance studies of $Zn_{1-x}Mn_xTe$. *J. Phys. Condens. Matter*. 1994. **6**, No. 6. P. 1261–1268. https://doi.org/10.1088/0953-8984/6/6/028.

Authors and CV

Dariya V. Savchenko: Doctor of Sciences in Physics and Mathematics, Associate Professor at the Department of General Physics and Modelling of Physical Processes of the National Technical University of Ukraine "Igor Sikorsky Kyiv Polytechnic Institute" and Scientist at the Department of Analysis of Functional Materials, Institute of Physics, CAS. The area of scientific interests of DrSc D.V. Savchenko includes magnetic resonance study in semiconductors, dielectrics and biomaterials. https://orcid.org/0000-0002-0005-0732

Maria K. Riasna: Master student at the Department of General Physics and Modelling of Physical Processes of the National Technical University of Ukraine "Igor Sikorsky Kyiv Polytechnic Institute". The area of scientific interests of M.K. Riasna includes magnetic resonance in diluted semiconductors.
E-mail: maria.ryasna@gmail.com

Maryna V. Chursanova: PhD in Physics and Mathematics, Associate Professor at the Department of General Physics and Modelling of Physical Processes of the National Technical University of Ukraine "Igor Sikorsky Kyiv Polytechnic Institute". The area of scientific interests of Dr M.V. Chursanova includes semiconductor physics.
E-mail: afina55@ukr.net,
https://orcid.org/0000-0001-6977-7473

Tetyana V. Matveeva: Dr, Associate Professor at the Department of General Physics and Modelling of Physical Processes, National Technical University of Ukraine "Igor Sikorsky Kyiv Polytechnic Institute". The area of her scientific interests includes solid state physics.
E-mail: tatianamatveeva27@gmail.com,
https://orcid.org/0000-0002-3374-9718

Nina A. Popenko: Doctor of Sciences in Radiophysics, Leading Researcher at the Radiospectroscopy Department, O.Ya. Usikov Institute for Radiophysics and Electronics, NASU. The area of her scientific interests includes radiospectroscopy of diluted semiconductors.
E-mail: ireburan@yahoo.com

Igor V. Ivanchenko: Doctor of Sciences in Radiophysics, Leading Researcher at the Radiospectroscopy Department, O.Ya. Usikov Institute for Radiophysics and Electronics, NAS of Ukraine. The area of his scientific interests includes radiospectroscopy of diluted semiconductors.
E-mail: ivanchenkoi534@gmail.com,
https://orcid.org/0000-0003-2540-4995

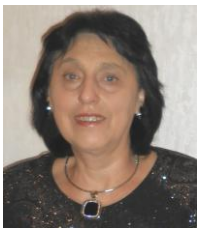

Ekaterina N. Kalabukhova: Doctor of Sciences in Physics and Mathematics, Leading Researcher at the Department of Optics and Spectroscopy, V. Lashkaryov Institute of Semiconductor Physics, NASU. The area of her scientific interests includes magnetic resonance in semiconductor and nanosized materials. E-mail: kalabukhova@yahoo.com, https://orcid.org/0000-0003-0272-9471

Authors' contributions

Savchenko D.V.: investigation, validation, software, formal analysis, data curation, writing – original draft, writing – review & editing.
Riasna M.K.: investigation, software, formal analysis, data curation (partially), writing – original draft, visualization.
Chursanova M.V.: conceptualization, writing – review & editing.
Matveeva T.V.: data curation (partially), writing – original draft.
Popenko N.A.: methodology, writing – review & editing, resources.
Ivanchenko I.V.: conceptualization, project administration, writing – review & editing.
Kalabukhova E.N.: supervision, writing – review & editing.

Дослідження кристалів $Cd_{1-x}Mn_xTe$ методами стаціонарного та імпульсного ЕПР з різним вмістом Mn

Д.В. Савченко, М.К. Рясна, М.В. Чурсанова, Т.В. Матвєєва, Н.О. Попенко, І.В. Іванченко, К.М. Калабухова

Анотація. Досліджено кристали телуриду марганцю кадмію ($Cd_{1-x}Mn_xTe$) (x < 0,001 та x = 0,02, 0,04, 0,1), вирощених за методом Бріджмена, із застосуванням стаціонарного та імпульсного електронного парамагнітного резонансу (ЕПР) у широкому діапазоні температур. Кристали $Cd_{1-x}Mn_xTe$ з x < 0,001 виявили спектр ЕПР ізольованого Mn^{2+} з $g_\perp = g_\parallel = 2{,}0074(3)$, $|A|_\perp = |A|_\parallel = 56{,}97\cdot10^{-4}$ см$^{-1}$, $|a| = 30.02\cdot10^{-4}$ см$^{-1}$, у той час як кристали $Cd_{1-x}Mn_xTe$ з x = 0,02…0,04 характеризуються двома поодинокими широкими ізотропними лініями ЕПР лоренцевої форми (g ~ 2,009 та g ~ 1,99) за рахунок присутності кластерів Mn різних розмірів. Спектр ЕПР кристалів $Cd_{1-x}Mn_xTe$ з x = 0,01 складається з однієї широкої лінії при g ~ 2,01 через вищий рівень однорідності, характерний для цих кристалів. Температурну залежність часів спінової релаксації для ізольованого центра Mn^{2+} у кристалах $Cd_{1-x}Mn_xTe$ з x < 0,001 описано з використанням процесу Орбаха для T_M^{-1} та Раманівського двофононного процесу для T_1^{-1}.

Ключові слова: ЕПР, час спінової релаксації, марганець, телурид кадмію марганцю.